BII-9

THE MECHANICAL PROPERTIES AS A FUNCTION OF TEMPERATURE AND FREE ELECTRON CONCENTRATION IN STOICHIOMETRIC TiNi, TiCo and TiFe ALLOYS

Frederick E. Wang*

ABSTRACT

Through single crystal X-ray and powder neutron diffraction methods, the crystal structures of TiFe, TiCo and TiNi have been determined. A unique "martensitic" transition has been found to exist in these alloys: TiFe - below 4°K, TiCo - at 38°K and TiNi - at 439°K. The unusual mechanical properties of TiNi, previously reported, are explained based on its 9 Å superstructure (substructure has a 3 Å repeat) and the "martensitic" transition.

On the other hand, the drastic change in mechanical properties, brittle → moderately ductile → extremely ductile, in going from TiFe → TiCo → TiNi can best be explained on the basis of the cohesive energy contributed by free electrons. This explanation points to the interesting possibility of raising the transition temperature, and hence the fracture strength, through addition of hydrogen as an interstitial electron donor. This possibility has been confirmed experimentally.

INTRODUCTION

A considerable amount of work on the equilibrium diagram (1-7) and on the structure of the intermediate phases (8-17) of the TiNi system has been previously reported. These efforts nevertheless failed to characterize the exact nature of the TiNi intermediate phase (18).

The unique mechanical properties of TiNi in the temperature range, 20°C ~ 100°C were first observed by Buehler et al (19-21). Some of these properties are: (a) high damping (acoustic) at room temperature and low damping at higher temperature, (b) unusually high endurance strength, (c) contraction of cold-drawn wire upon heating, (d) high ductility (tensile elongation in excess of 20%), and (e) "memory" effect (if a wire or sheet of this alloy is deformed at room temperature, it will regain its original shape when heated to a higher temperature).

---

*U. S. Naval Ordnance Laboratory, White Oak, Maryland, U. S. A.

Through single crystal X-ray and powder neutron diffraction studies*, the crystal structure of TiNi has been determined** and the existence of a "martensitic" transition (without crystallographic transformation) has been confirmed. In this paper, a mechanism for this transition, based on the crystal structure of TiNi, is described which explains these unusual mechanical properties associated with the alloy in a qualitative manner.

In addition, the present work covers the ternary phases, Ti-Ni-Co and Ti-Co-Fe, formed by replacing nickel with cobalt and iron in stoichiometric TiNi.

EXPERIMENTAL

Alloy Preparation

The alloy specimens employed in this investigation were prepared by non-consumable arc-melting. A stable arc for melting was maintained by the use of low pressure dry argon gas. Several remelts were performed on each alloy to insure chemical homogeniety. The alloys were prepared from Mond carbonyl nickel shot (99.9 + % Ni), electrolytic cobalt (99.9 + % Co), electrolytic iron (99.96 % Fe) and DuPont high purity titanium sponge (99.6 % Ti) having a Brinnel hardness number of approximately 80. The lot of titanium sponge used contained 0.07 wt. % Fe as a known impurity. The maximum amounts of the other impurities in Ti sponge of this type were about 0.15 wt. % for combined interstitial elements, plus Mn up to 0.05, Mg up to 0.08 and Si up to 0.04 wt. %.

Composition monitoring was accomplished principally by determining the weight loss during melting. In every case, the weight of the final alloy varied from the charge weight by no more than 0.1%.

Determination of the Transition Temperature and the Hardness of the Alloys

Since the acoustic damping characteristic changes drastically above and below the transition, the majority of the transition temperature were determined by striking bars of the various alloys (approximately 1.5 cm. in diameter and 10 cm. in length) and noting the sharp change in their ringing characteristics. These determinations were complemented and confirmed by X-ray diffraction techniques. Hardness determinations were made by using a diamond pyramid indenter in a standard Tukon microhardness tester at the loads of 500 gm. ~ 3,000 gm.

*TiNi single crystals have been grown by the modified "strain-anneal" technique described in reference 22.

**The details of the TiNi crystal structure determination has been reported by F. E. Wang, W. J. Buehler and S. J. Pickart, J. Appl. Phys. Vol. 36, p 3232 (1965).

RESULTS AND DISCUSSION

The Crystal Structure of TiNi above the Transition Temperature

The TiNi short range crystal structure above the transition consists of two interpenetrating simple cubic lattices whose linear atomic sequences along the $\bar{a}$, $\bar{b}$ and $\bar{c}$ axes are -Ti-Ti-Ni-Ti-Ti- and -Ni-Ni-Ti-Ni-Ni- respectively as shown in Fig. 1. This short range crystal structure has rhombohedral symmetry and alternate layers of Ti and Ni atoms on successive (111) planes. As shown in Fig. 2, there are four possible orientations of the structure in which the Ti and Ni atom layers lie on successive (111), ($\bar{1}\bar{1}1$), ($\bar{1}11$) and ($1\bar{1}1$) planes. In each case, the linear atomic sequence remains the same. It is observed in this figure that the first and the fourth layer of types I and II are identical. Moreover, the second layer of type I is identical to the third layer of type II and conversely, the third layer of type I is identical to the second layer of type II. Therefore, if the layer stacking sequence is designated as ABCABC for type I, in type II the sequence must be ACBACB. This demonstrates the fact that the four different orientations can also be considered as stacking faults.

The long range TiNi cubic crystal structure consists of regions of different orientation which are statistically distributed and bounded by antiphase boundaries.

Cooperative Atomic Movements at and below the Transition Temperature

The shear-like cooperative atomic movements in TiNi at and below the transition temperature take place on {110} planes as shown in Fig. 3. The approximate directions of the movements are in [111] and indicated by arrows. The planes on which the atoms would eventually come to rest at the M_f temperature are indicated by dotted lines. Single crystal X-ray studies below the transition temperature (down to -70°C) indicate that the M_f temperature (below which, the matrix consists entirely of "martensites") for TiNi is far below -70°C and that the magnitudes of these movements are inversely proportional to the absolute temperature. This implies that the atomic positions below the transition temperature are not as rigidly fixed as they are above the transition temperature. This observation, together with the fact that near-stoichiometric TiNi alloys are extremely ductile below the transition temperature, strongly suggests that metallic bonding dominates the covalent (directional) bonding below the transition temperature. This postulate offers a reasonable explanation for the high damping below the transition temperature and conversely, the low damping above the transition temperature. Consequently, the interatomic distances at progressively lower temperatures below the transition temperature should approach

those found in the pure Ti and Ni metals. As shown in Fig. 3, the atoms separated by 3.0 Å and 2.6 Å above the transition temperature move cooperatively into new positions below the transition temperature such that the interatomic distances do approach those of pure metallic states*.

The Ternary Phases: $Ti(Ni_x, Co_{1-x})$ and $Ti(Co_x, Fe_{1-x})$

All ternary phases, $Ti(Ni_x, Co_{1-x})$ and $Ti(Co_x, Fe_{1-x})$ formed by replacing Ni with Co and Fe, have crystal structures similar to TiNi and exhibit the CsCl-type diffraction pattern** above their respective transition temperatures. Assuming the number of free electrons contributed by Ti, Fe, Co and Ni in their alloys to be 4, 8, 9 and 10 (number of outer electrons in d shell) respectively, the transition temperatures plotted as a function of the free electron concentrations (number of free electrons per atom) in these alloys is a smooth curve as shown in Fig. 4. This curve indicates that the martensitic-type transition observed in TiNi is not unique to this compound alone, but is prevalent to those alloys which are formed by the first transition elements and whose crystal lattice is of the CsCl-type.

The fracture energy and the hardness as a function of the composition of the ternary alloys, $Ti(Ni_x, Co_{1-x})$ and $Ti(Co_x, Fe_{1-x})$ are given in Figs. 5-(a) and 5-(b) respectively. The drastic change in mechanical properties, (i.e., brittle → moderately ductile → extremely ductile) in going from TiFe → TiCo → TiNi is noteworthy. Since all the ternary phases investigated here have the same crystal structure with about the same lattice constant (TiFe - 2.98 Å, TiCo - 2.99 Å and TiNi - 3.00 Å) the characteristic covalent bonding involved should be the same. The only variant is therefore the free electron concentration.

Since a free electron in an ordinary metal contributes, on the average, one to two electron volts of cohesive energy (24) in holding atoms together, the mechanical property change observed in TiFe → TiCo → TiNi, can best be explained based on the free electron concentration. This explanation is well supported by the following experiments.

Introduction of Hydrogen into TiNi and its Effect

A strip of TiNi (20 x 1.5 x 0.05 cm.) was encapsulated in a vycor tube and connected to a vacuum system (blank off pressure - 10^{-7} mm).

*The interatomic distances of Ti and Ni in their metallic states are 2.89 and 2.49 Å respectively (INTERATOMIC DISTANCES, The Chemical Soc., Burlington House, London, 1958).

**This is in agreement with the finding of Starke, Cheng and Beck (ref. 23). However, these authors were not aware of the unique "martensitic" transitions in these alloys.

The tube and sample were sustained at 900°C, at pressure of 10^{-7} mm for 24 hours to insure cleanliness. Following a free cool to room temperature, hydrogen gas was then introduced to a pressure of 80 microns. Absorption of hydrogen by TiNi was monitored by a continuous measurements of the hydrogen pressure in the system. The equilibrium pressure at a given temperature was established within minutes and is plotted against the temperature in Fig. 6. The curve indicates no absorption of hydrogen by TiNi up to about 500°C and a maximum absorption at about 625°C. Upon cooling to room temperature, over 40 microns of hydrogen gas pressure drop was observed; this is approximately equivalent to 150 ppm concentration of hydrogen in the TiNi strip.

Hardness measurements made on hydrogen treated TiNi strip indicates an R_A of 41.0 compared to 43.5 for a control TiNi strip. This decrease though small is accompanied by an experimentally confirmed elevation in the transition temperature. Therefore, it seems reasonable that this decrease in hardness is directly related to an increase in the free electron concentration as shown in Fig. 5-(b).

ACKNOWLEDGEMENT

Many valuable discussions with Mr. W. J. Buehler in the course of this investigation and the able assistance rendered by Mr. A. M. Syeles in all phases of the experimental work are gratefully acknowledged.

REFERENCES

1. Vogel, R. and Wallbaum, H. J., Arc. Eisenhuttenw, Vol. 12, 299 (1938).
2. Wallbaum, H. J., ibid., Vol. 14, 521 (1940).
3. Taylor, A. and Floyd, R. W., J. Inst. Metals, Vol. 80, 577 (1951).
4. Margolin, H., Ence, E. and Nielsen, J. P., Trans. Met. Soc. AIME, Vol. 197, 243 (1953).
5. Long, J. R., Hayes, E. T., Root, D. C. and Armantrout, C. E., U. S. Bur. Mines Rept. Invest., 4463 (1949).
6. Purdy, G. R. and Parr, J. G., Trans. Met. Soc. AIME, Vol. 221, 636 (1961).
7. Poole, D. M. and Hume-Rothery, W., J. Inst. Metals, Vol. 83, 473 (1954-55).
8. Taylor, A. and Floyd, R. W., Acta Cryst., Vol. 3, 285 (1950).
9. Laves, F. and Wallbaum, H. J., Naturwissenschaffen, Vol. 27, 674 (1939).

10. Dewez, P. and Taylor, J. L., Trans. Met. Soc. AIME, Vol. 188, 1173 (1950).

11. Rostoker, W., Trans. Met. Soc. AIME, Vol. 191, 1203 (1951).

12. Laves, F. and Wallbaum, H. J., Z. Krist, Vol. 101, 78 (1939).

13. Phillip, T. V. and Beck, P. A., Trans. Met. Soc. AIME, Vol. 209, 1269 (1957).

14. Stuwe, H. and Shimomura, Y., Z. Metallk, Vol. 51, 180 (1960).

15. Pietrokowsky, P. and Youngkin, F. G., J. Appl. Phys., Vol. 31, 1763 (1960).

16. Mueller, M. H. and Knott, H. W., Trans. Met. Soc. AIME, Vol. 227, 674 (1963).

17. Gilfrich, J. V., "Proceedings of the Eleventh Annual Conference on Application of X-ray Analysis", Aug. 1963.

18. Hansen, M., "Constitution of Binary Alloys", McGraw-Hill Book Co., Inc., New York, (1958).

19. Buehler, W. J. and Wiley, R. C., Trans. Quart. ASM, Vol. 55, 269 (1962).

20. Buehler, W. J., Gilfrich, J. V. and Wiley, R. C., J. Appl. Phys., Vol. 34, 1475 (1963).

21. Buehler, W. J., "Proceedings Seventh Navy Science Symposium" (ONR-16, Vol. 1, unclassified, Off. of Tech. Serv., U. S. Dept. of Commerce), May 1963.

22. Wang, F. E., Syeles, A. M., Clark, W. L. and Buehler, W. J., J. Appl. Phys., Vol. 35, 3620 (1964).

23. Starke, E. A. Jr., Cheng, C. H. and Beck, P. A., Phys. Review, Vol. 126, 1746 (1962).

24. Ziman, J. M., "Electrons in Metals", Taylor & Francis Ltd. (1962).

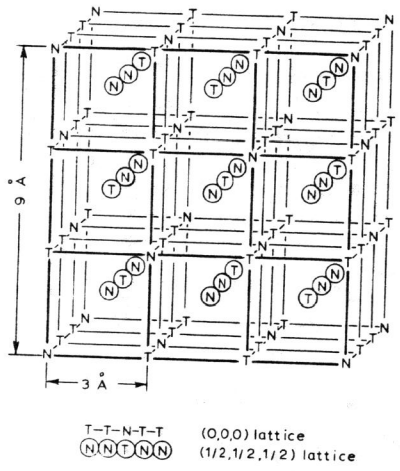

Fig. 1 - The 9 Å superstructure in TiNi based on the atomic linear sequences of -Ti-Ti-Ni-Ti-Ti- and -Ni-Ni-Ti-Ni-Ni-; T and N stand for titanium and nickel atoms respectively.

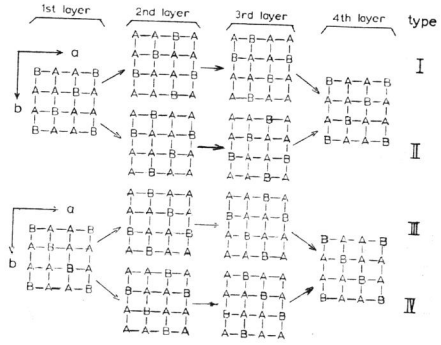

Fig. 2 - The four possible structure of TiNi are exemplified, based on the linear atomic sequence of -A-A-B-A-A- (where A represents Ti and B represents Ni or vice versa). Successive layers of A and B lie on (111), $(\bar{1}\bar{1}1)$, $(1\bar{1}1)$ and $(\bar{1}11)$ respectively in types I, II, III and IV.

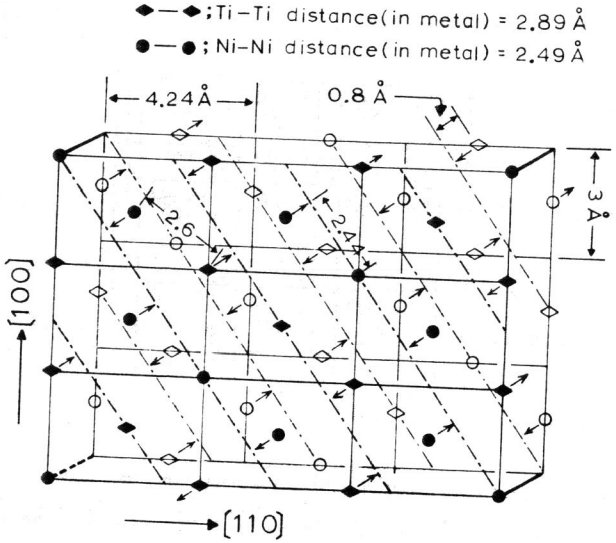

Fig. 3 - The shear-like cooperative atomic movements on {110} planes at and below the transition temperature in TiNi. The arrows indicate the approximate directions of the movements; the broken lines indicate the planes, the atoms should reach at the M_f temperature. Solid circles and diamonds designate Ni and Ti atoms on the plane in front, where open circles and diamonds designate the respective atoms on the plane behind.

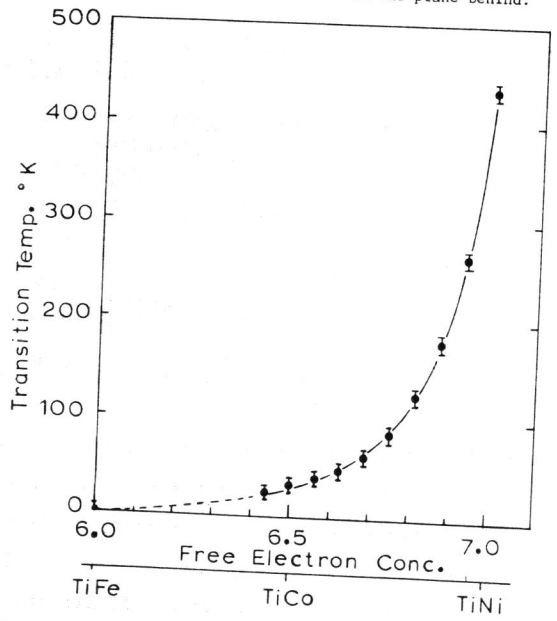

Fig. 4 - The "martensitic" transition temperatures vs compositions in ternary phases, Ti (Ni_x, Co_{1-x}), Ti (Co_x,Fe_{1-x}) therefore, vs free electron concentration.

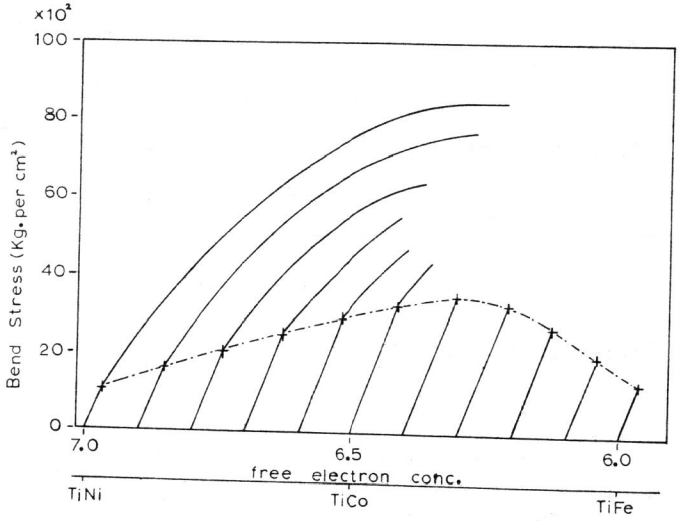

Fig. 5-(a) Bend Stress-Strain curves of the Ti-Ni-Co, Ti-Co-Fe ternary alloys with the "CsCl"-type structure. The measurements were made on a Baldwin Universal Tester, using 0.64 cm/min loading rate and at room temperature. All samples were in the arc-cast condition and given a stress-relief anneal at 800°C for one hour prior to testing.

+ Indicates the elastic limit in each sample.

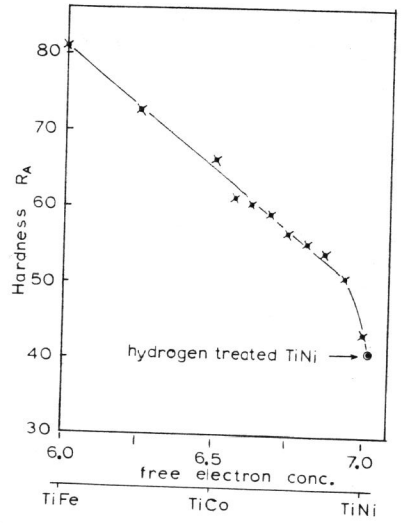

Fig. 5-(b) - Hardness vs. composition in ternary phases, $Ti(Ni_x,Co_{1-x})$, $Ti(Co_x,Fe_{1-x})$, therefore, vs. free electron concentration.

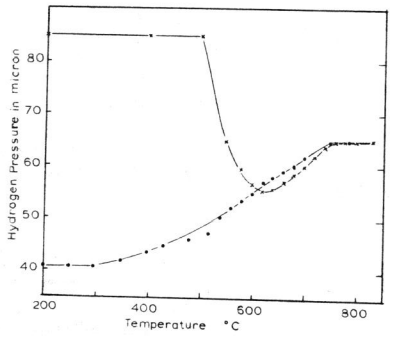

Fig. 6 - Hydrogen pressure (in microns) vs. temperature obtained in the hydrogen treatment of TiNi. x and • indicate the pressure in the course of heating and cooling respectively.